# The Ram Energy Distribution Detector (REDD)
# A New Neutral Wind Instrument for Nano-Satellite Platforms

Lee Kordella[1], Gregory Earle[1], Grant Roth[1], Stephen Noel[1], Robbie Robertson[2], Ryan Davidson[3], Christopher Holland[4]
[1]Virginia Tech, [2]Cubic Aerospace, [3]Utah State University, [4]SRI International

## Motivation

Virginia Tech has developed an in-situ sensor called the Ram Energy Distribution Detector (REDD, pronounced red-dee) to measure the neutral density, changes in the neutral temperature, the light/heavy composition ratio, and the ram velocity of the neutral gas in the frame of reference of an orbital spacecraft. These are critically undersampled parameters for studying ion-neutral coupling effects that are relevant to a host of geophysical effects in Earth's thermosphere/ionosphere system, including scintillation and equatorial spread-F. Neutral density, temperature, and wind measurements are also critical parameters for understanding spacecraft drag in planetary atmospheres, so the REDD sensor could also be used to better understand such effects in the atmospheres of Mars and other planetary bodies. Here we present the results of subsystem validation through laboratory vacuum testing.

## The REDD Sensor

The operational concept of the REDD instrument is based on the Ram Wind Sensor (RWS) [1] which was flown on the Communications/Navigation Outage Forecasting System (C/NOFS) satellite. REDD is a next generation neutral wind sensor designed for reduced size, weight and power (SWaP) applications in the growing small satellite community. Figure 1 displays a computer generated mechanical cross-section, SIMION® charged particle simulation and the final assembly of the REDD device. The key components labeled include biased extraction plates to reject background space plasma, an internal ionization source, a retarding potential analyzer (RPA) grid-stack for particle diagnostics and a high gain microchannel plate (MCP) detector for ion collection. The process flow for the instrument is summarized in the flowchart below.

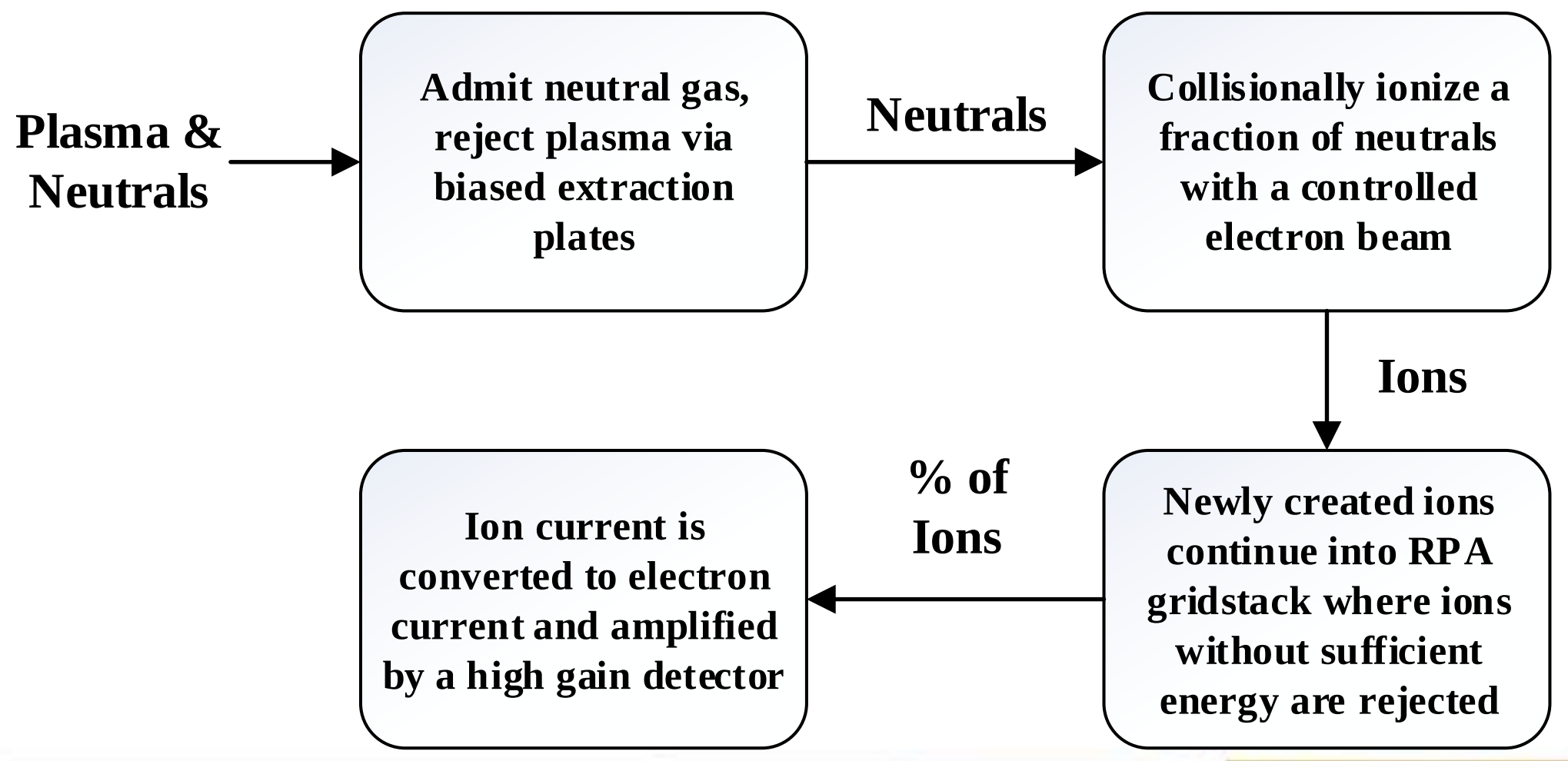

**Plasma & Neutrals** → **Admit neutral gas, reject plasma via biased extraction plates** → **Neutrals** → **Collisionally ionize a fraction of neutrals with a controlled electron beam** → **Ions** → **Newly created ions continue into RPA gridstack where ions without sufficient energy are rejected** → **% of Ions** → **Ion current is converted to electron current and amplified by a high gain detector**

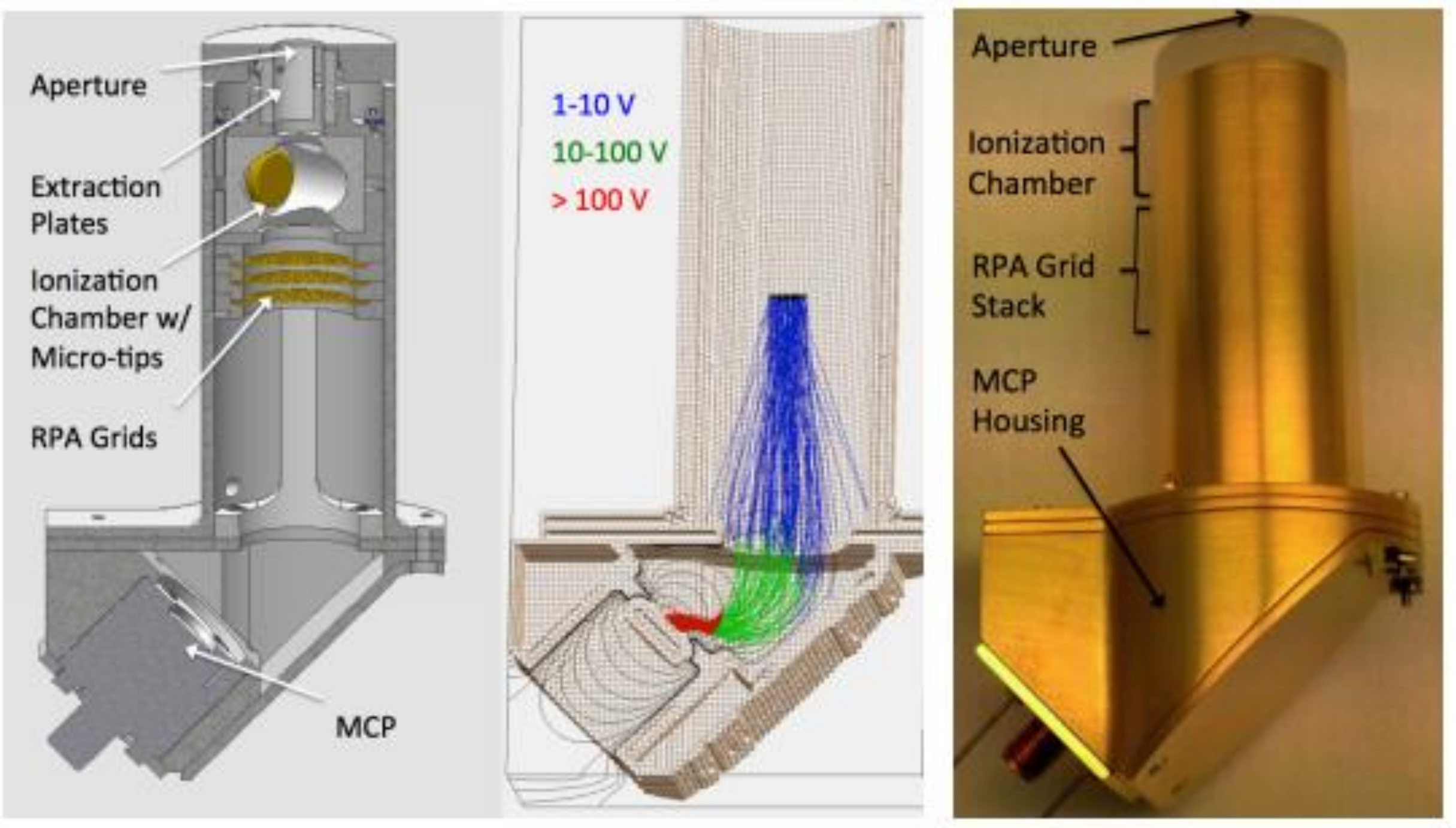

*__Figure 1__ – The left panel shows a cross-section of the REDD device and labels the key subsystems. The middle panel shows the results of a simulation study to trace ion trajectories from the grid stack to the front surface of the MCP. The right panel shows the assembled sensor with corresponding labels of the hidden components*

## Testing Procedure

Because a neutral beam system capable of flowing oxygen gas at hypersonic velocities in vacuum was not available it was not possible to perform true end-to-end testing on the REDD system. Instead, separate functional tests were performed to validate each subsystem, as described below:

1. Ion source testing – the REDD sensor was mounted in vacuum and the REDD internal ionization source was energized to verify that the MCP current scales in proportion to the neutral chamber pressure. The grids were biased to draw ions out of the ionization chamber, since the neutral particles had no directed velocity
2. RPA testing – By injecting ions from an independent plasma source into the aperture of the REDD sensor it was confirmed that the RPA grid stack within REDD is capable of measuring a current-voltage (IV) characteristic indicative of the energy distribution of the ions flowing into the system.

## Ion Source Test

A key difference between the RWS and REDD sensors is the incorporation of a Spindt-type field emitter [2] developed by SRI International as the REDD ionization source in place of the hot filament utilized by the RWS. Spindt-type field emitters consist of small, sharp, conductive cones that form a large-area field electron source, as shown in Figure 2. The emitter tips are driven to a negative potential with respect to a forward counter-electrode which acts to create a high electric field. The resulting electron emission from metals under electric fields is characterized by the Fowler-Nordheim relationship [3].

- ❖ The primary advantage to the micro-tip emitter solution as opposed to a filament electron source is the reduction in power consumption by a factor of ~1,000. This improvement is highly advantageous for applications in the growing small satellite community. An upcoming orbital mission will test these emitters as part of a technology demonstration instrument on the LAICE CubeSat mission [4].
- ❖ The micro-tips are subject to various failure modes including polymer contamination (Figure 2) and filamentary shorts between the electrodes. These factors can lead to degraded emission capability, instability and ultimately failure of the device. Contamination effects can be mitigated through thermal conditioning processes as recommended by SRI. Figure 3 displays the improvement of emission characteristics after sufficient thermal conditioning.

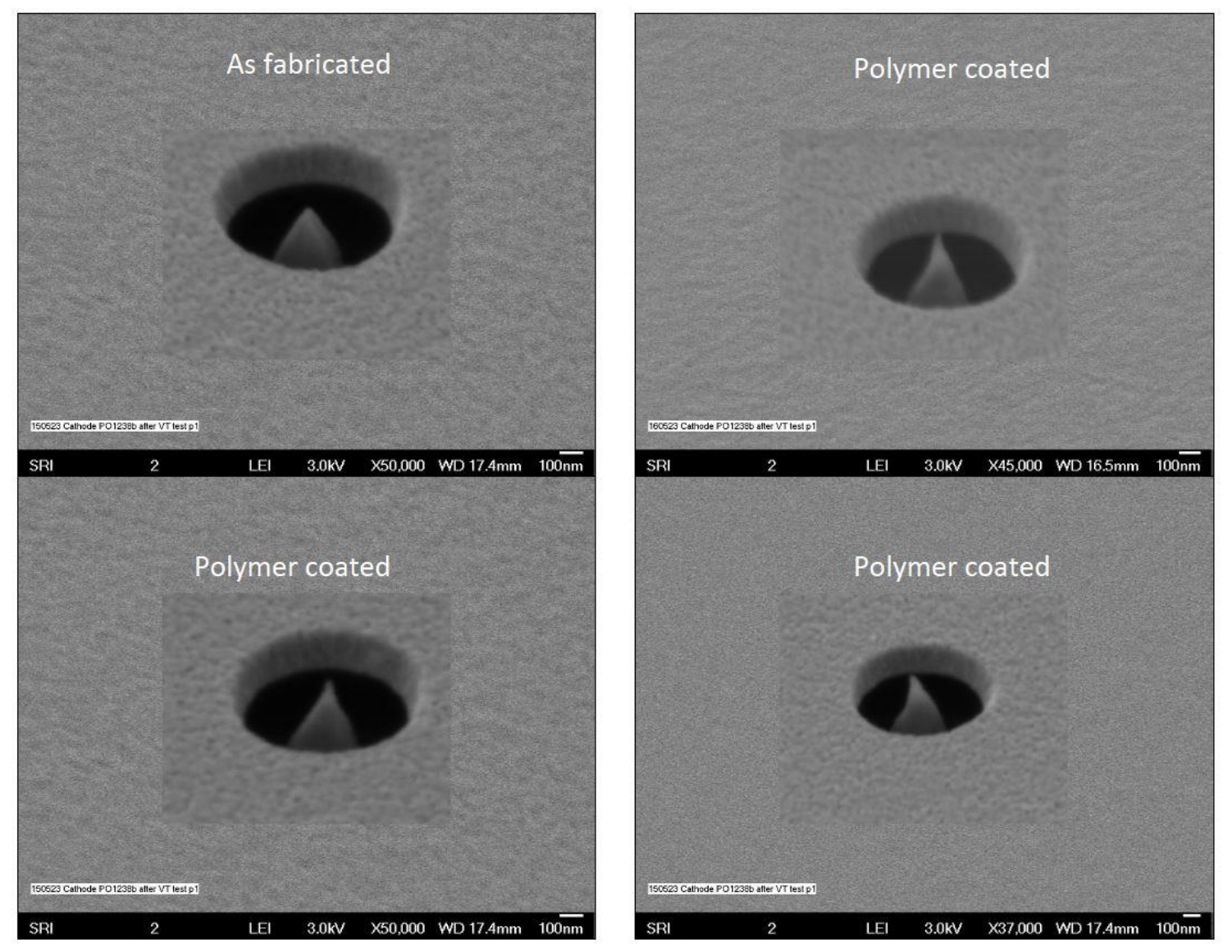

*__Figure 2__ – Electron microscope images of uncontaminated and polymer contaminated micro-tip emitters.*

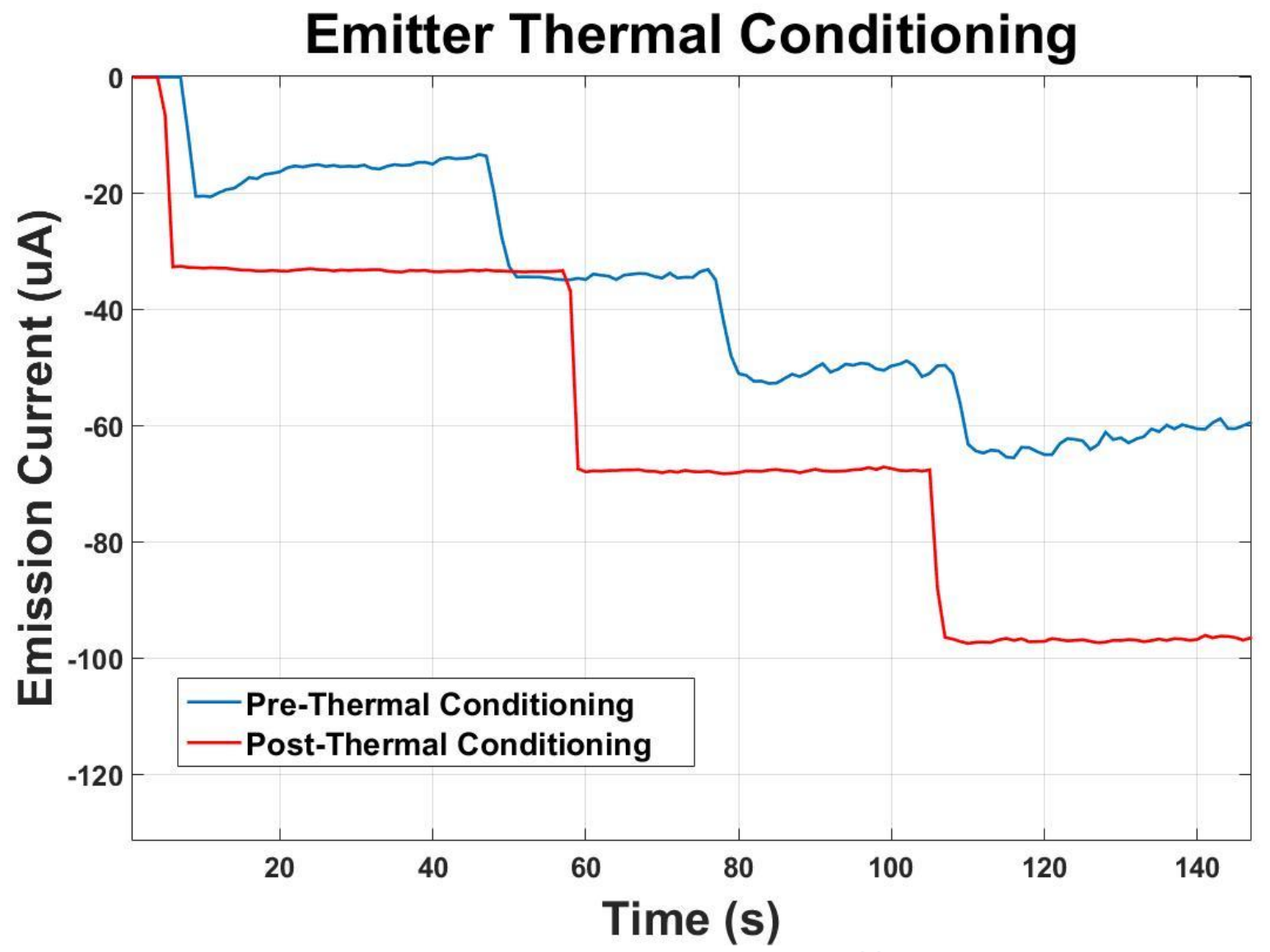

*__Figure 3__ – Thermal conditioning effect on electron emission stability. The step function like behavior corresponds to desired emission current levels .*

Figure 4 displays the test apparatus in a vacuum chamber for the pressure sensitivity test. Because of geometrical and low melting point material constraints of the device, the required thermal conditioning was accomplished using an external halogen bulb and a radiant energy collector plate in contact with the emitter tip biasing lead on the microtip device.

The data shown in Figure 5 represent the variation in the ionization produced by the micro-tip emitter source as a function of the background neutral pressure in the vacuum chamber. The data are normalized by the emission current in order to show the pressure dependence independent of emission fluctuations. The error bars represent variations over 30 data points recorded at a 1 second cadence.

- ❖ The empirical data are roughly linear across the pressure range, as expected.
- ❖ Deviations from linearity occur at low pressures. Possible explanations include increasing space charge effects or changes in the physical characteristics of the ionization region within the instrument as collisional ionization efficiency decreases. Due to base pressure limitations of the vacuum system, we were not able to further investigate these possibilities.

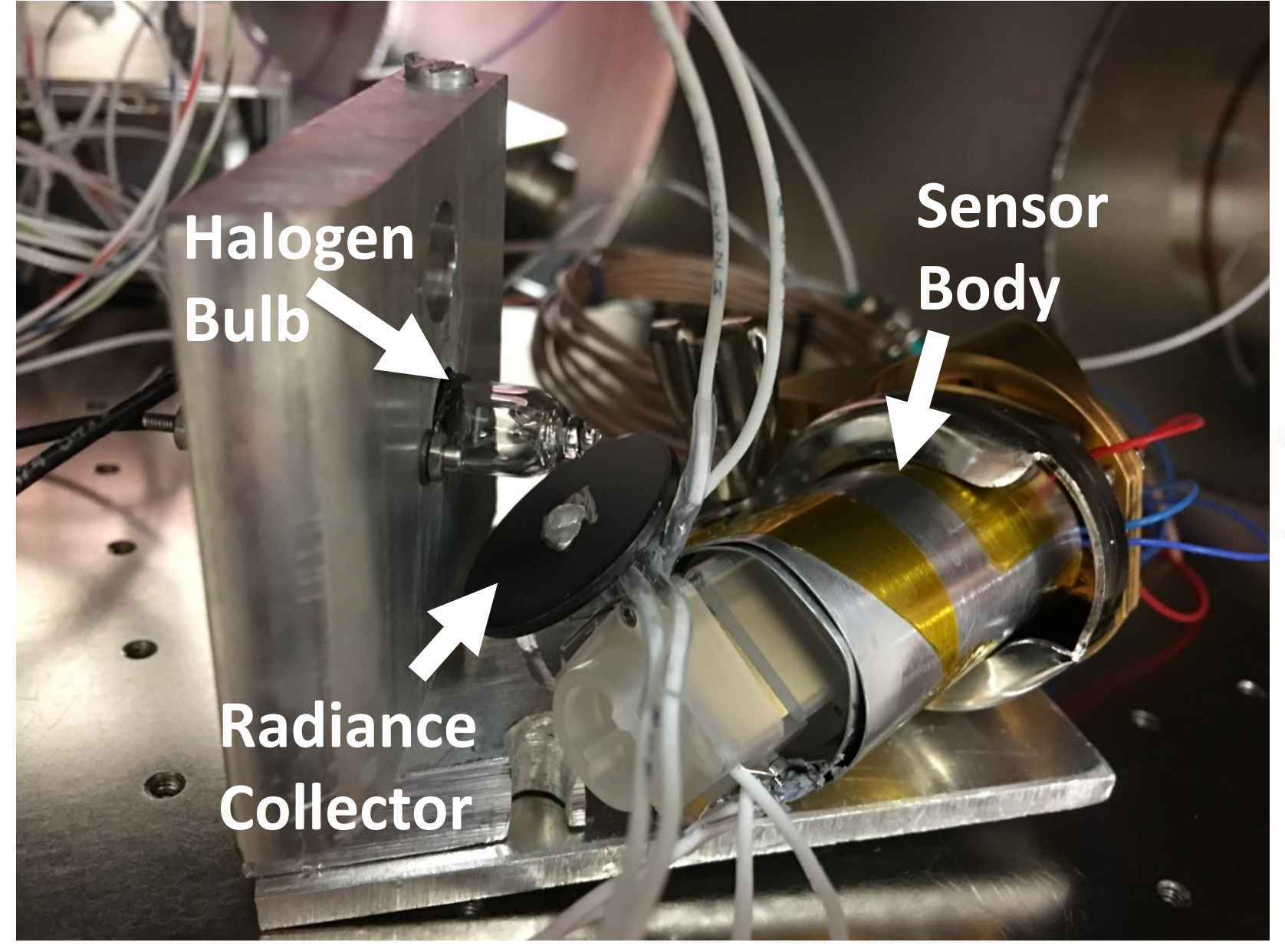

*__Figure 4__ – REDD ion source testing vacuum chamber assembly. Emitter thermal conditioning is accomplished by the collection of radiant energy by a carbon coated disc (seen in black) which is in electrical contact with the emitter tip biasing lead.*

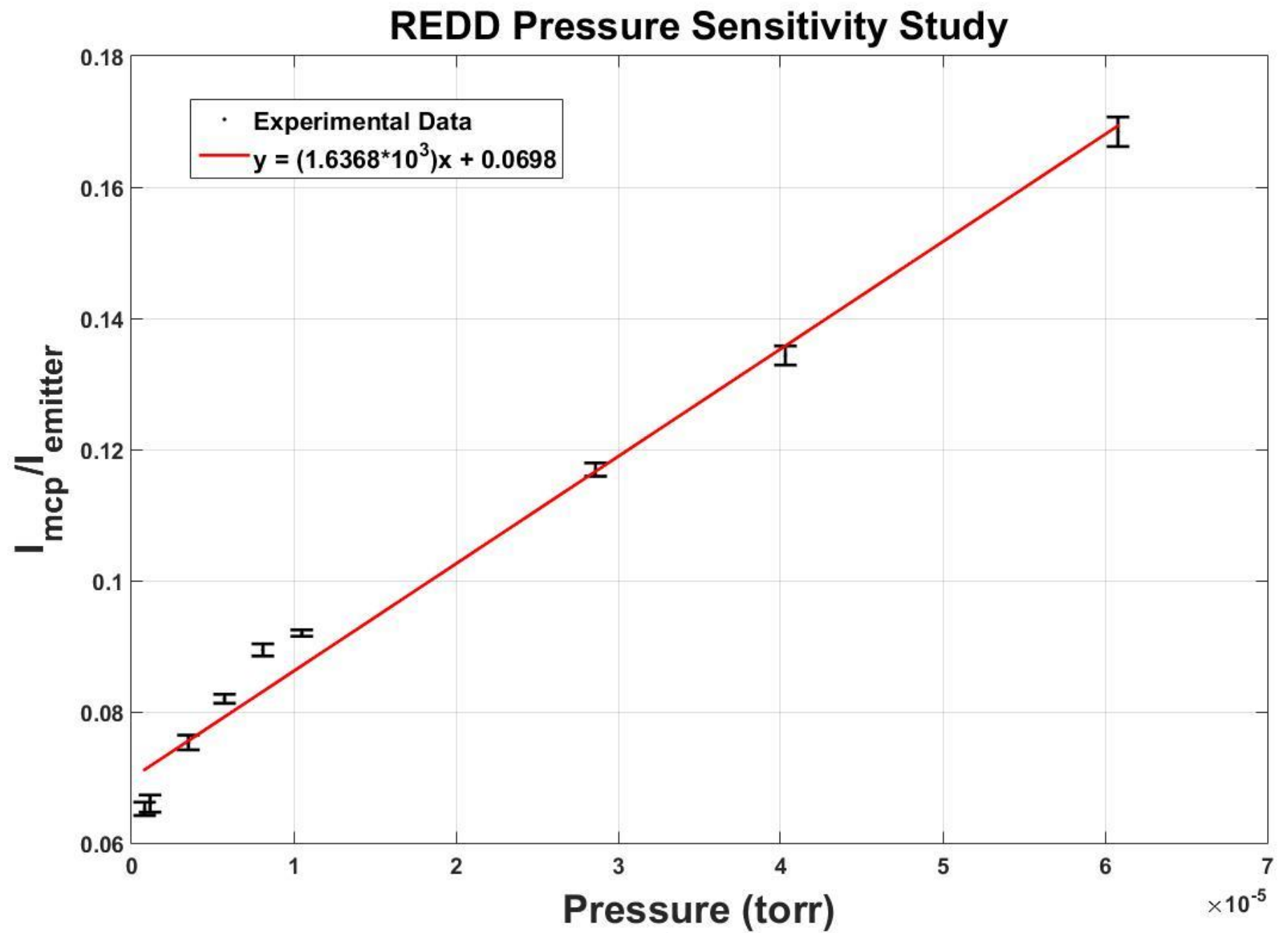

*__Figure 5__ – The ratio of current measured on the microchannel plate (MCP) to the microtip emitter current is plotted over a pressure range of ~$10^{-6}$ to $6 \times 10^{-5}$ Torr of dry nitrogen gas.*

## RPA Test

RPAs are simple plasma diagnostic instruments with a rich flight heritage. They are comprised of a series of flat, electrically conductive grids in a stacked parallel-plane configuration. Most of these grids are held at constant potentials, but one referred to as the retarding voltage (RV) grid is driven by a positive, periodic sweeping voltage. The RV grid creates a time varying energy barrier that limits ion throughput to those with sufficient energy. Curve fitting techniques using the resulting current and retarding voltages provide measurements of particle density, temperature, velocity and the light/heavy ion species composition ratio [5].

For this test the REDD instrument was placed in front of an external ion source (Figure 6) capable of flowing an ion beam with kinetic energies and densities similar to those expected in low Earth orbit (LEO). Figure 7 displays the resulting experimental IV characteristic. It can be clearly seen that increasing the retarding potential successfully suppresses the throughput current to the MCP detector, as expected.

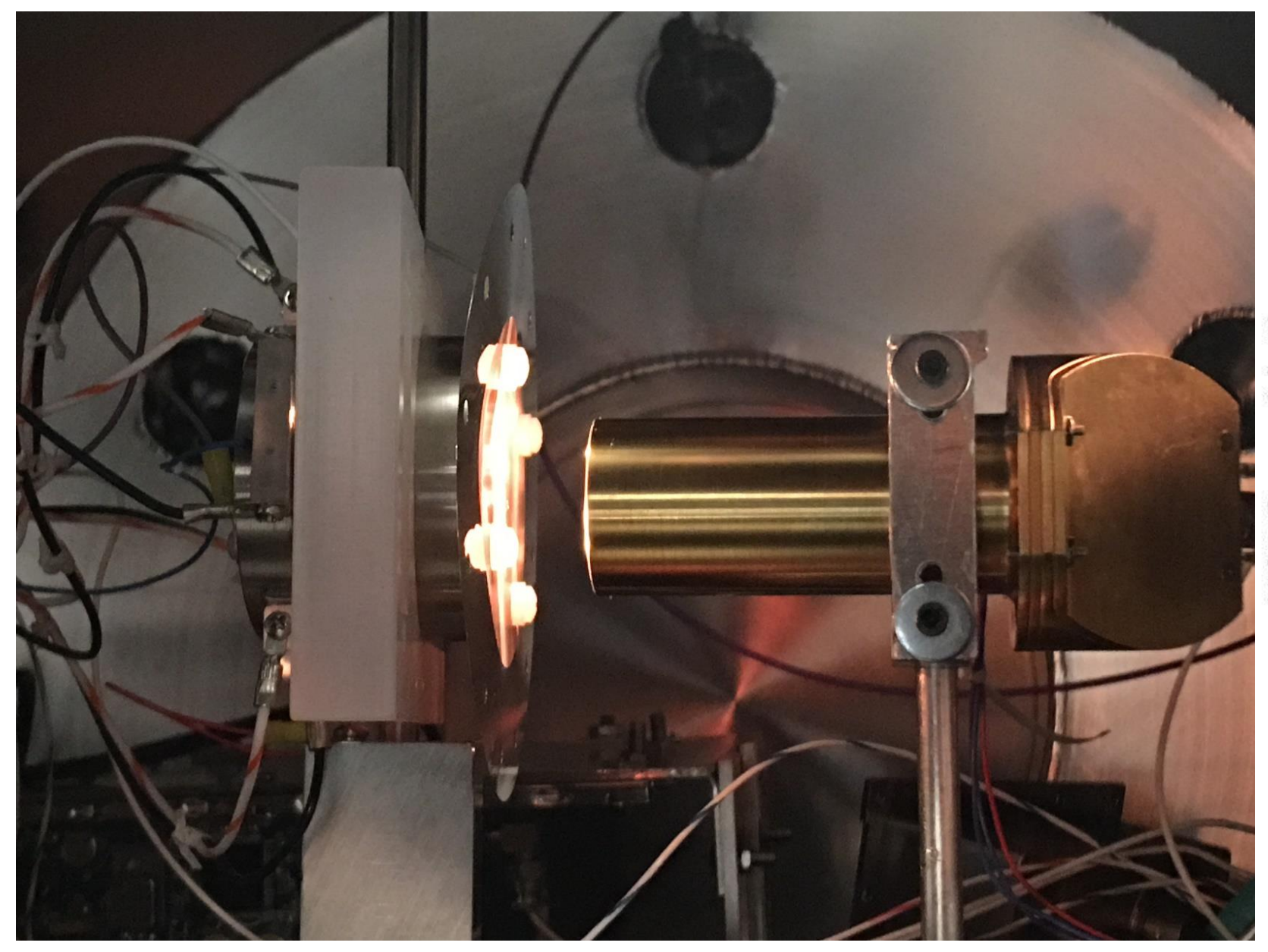

*__Figure 6__ – REDD RPA vacuum chamber test assembly. The REDD instrument is placed in front of an independent, hot-filament ion source capable of producing an ion beam with LEO characteristics.*

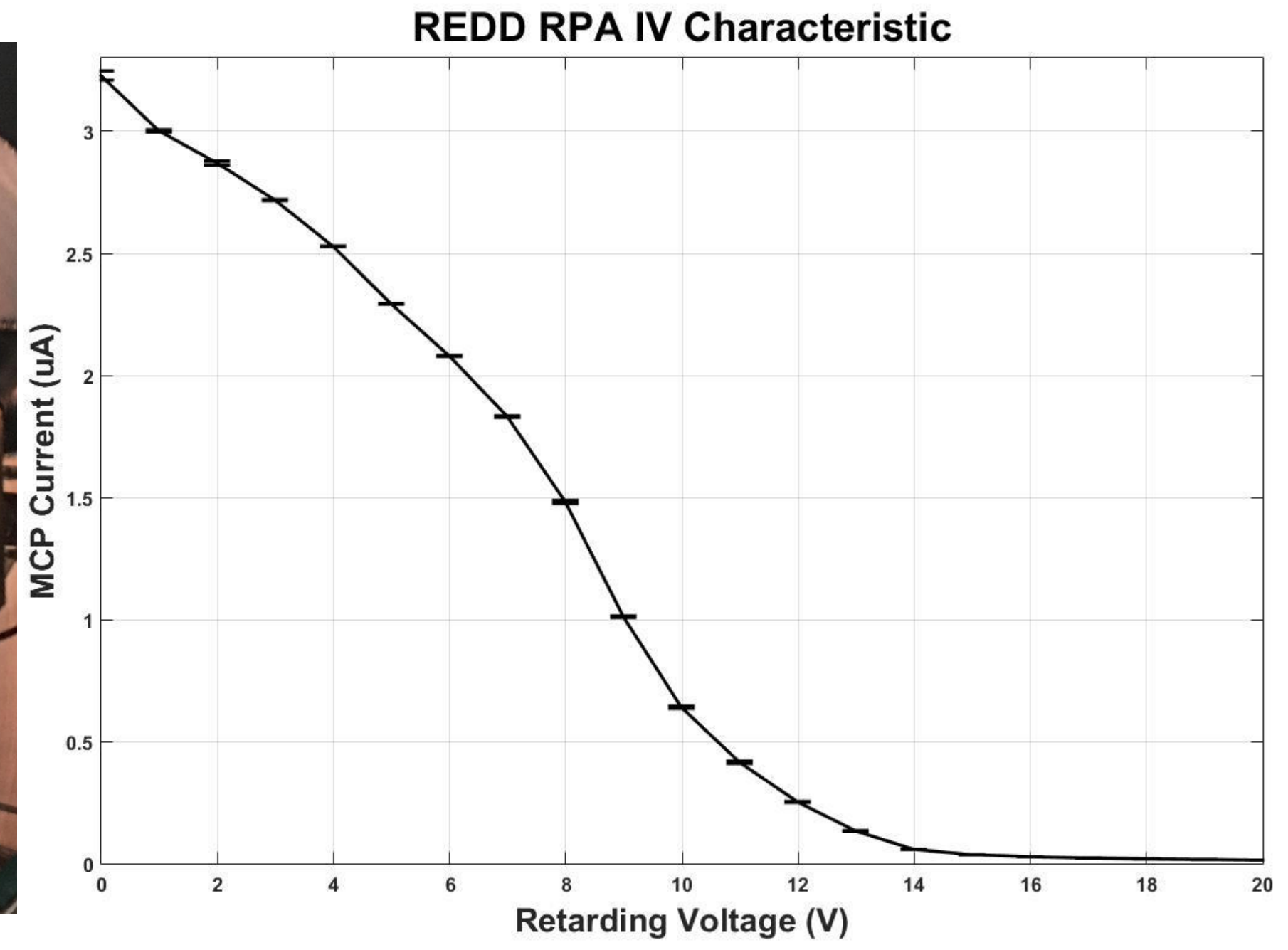

*__Figure 7__ – An RPA IV curve generated in vacuum by placing an independent ion source in front of the REDD aperture, and disabling the ion source and extraction plates within the REDD system. Note the very small error bars, indicating consistent performance over many trials.*

## Conclusions and Future Research

- ❖ Through the work reported here we have developed the REDD system from the concept stage through the level of subsystem tests in a relevant laboratory environment, thereby raising the technical readiness level (TRL) of the REDD system to 6.
- ❖ Mechanical improvements to accommodate in-flight thermal conditioning of emitters should be implemented, including the replacement of low-melting-point insulators with machinable ceramics, and the inclusion of a local heat source.
- ❖ The final step in validating REDD is to run all the subsystems simultaneously in a vacuum system that contains a calibrated neutral beam source, preferably one that can flow oxygen gas at speeds of several thousand meters per second. This experiment has been approved under a NASA cooperative agreement notice (CAN) to take place at the Marshall Space Flight Center atomic oxygen beam facility (AOBF) later this year.

## Acknowledgements

This research was supported by Air Force Research Lab small business innovative research (SBIR) grant AF121-066, and carried out with management oversight from Drs. Ted Beach and Odile Clavier from Creare LLC. The authors thank Drs. Cheryl Huang, John Ballenthin and Patrick Roddy for supporting and reviewing this project at AFRL.

## References

1. Earle, G. D., et al. "A new satellite-borne neutral wind instrument for thermospheric diagnostics." *Review of Scientific Instruments* 78.11 (2007): 114501.2. W. Hwang, Y.-K. Kim and M.E. Rudd, J. Chem. Phys. 104, 2956 (1996).
2. Brodie I., and C. A. Spindt, Vaccum Microelectronics, in *Adv. in Electronics and Electron Physics*, 83, 1, 1992.
3. Brodie, I., and P. R. Schwoebel, Vacuum Microelectronic Devices, *Proc. IEEE, 82*, 1006, 1994.
4. Westerhoff, John, et al. "LAICE CubeSat mission for gravity wave studies."*Advances in Space Research* 56.7 (2015): 1413-1427.
5. Knudsen, W. C. (1966), Evaluation and demonstration of the use of retarding potential analyzers for measuring several ionospheric quantities, J. Geophys. Res., 71(19), 4669–4678